 

PACS numbers: 42.55.Tv; 42.70.Qs
DOI: 10.1070/QE2015v045n02ABEH015581

# Propagation of frequency-modulated pulses in active one-dimensional photonic crystals

I.O. Zolotovskii, D.A. Korobko, V.A. Ostatochnikov

*Abstract.* **The propagation of frequency-modulated pulses in one-dimensional photonic crystals with gain is considered. A correct expression is derived for the delay time of the pulse maximum. This expression takes into account the input pulse characteristics: duration, frequency modulation and spectrum position in the photonic band gap. The analytical results are basically in agreement with the results of numerical simulation. The influence of gain in the photonic-crystal structure is considered. It is shown that the parameters of a transmitted pulse can be controlled by changing the input-pulse frequency modulation.**

***Keywords:*** *one-dimensional photonic crystals, frequency-modulated pulses, delay time.*

## 1. Introduction

Tunnelling (transmission of a quantum particle through a potential barrier the height of which exceeds the particle energy) is a fundamental quantum effect. When determining the tunnelling time, the key problem is to find out the particle velocity in the region where its momentum has an imaginary value [1, 2]. Calculation of the particle tunnelling time using the stationary-phase method leads to the well-known Hartman paradox, according to which the tunnelling time does not exceed some finite value. If the barrier is sufficiently thick, particles or wave packets may have superluminal tunnelling velocities [2, 3].

Some ways to explain the Hartman paradox have been discussed for a rather long time; this discussion includes the solution of the quite classical optical problem of transmission of electromagnetic waves through macroscopic photonic barriers [2, 4–12]. This problem is also of applied importance: the possibility of controlling wave velocity or delay time of a wave packet propagating through a barrier [13, 14] can be used in some optoelectronic devices.

In the last decade researchers have paid much attention to one-dimensional photonic crystals (PCs), which are layer-periodic structures based on different materials. Due to the periodic modulation of the refractive index in these structures, their spectrum has a band gap, within which the transmittance is close to zero, and light incident on them is almost completely reflected [15–17]. Propagation of wave packets within the band gap is in essence similar to tunnelling, because the time-independent Schrödinger equation is similar to the Helmholtz equation, which describes wave propagation in one-dimensional PCs.

A number of experiments on propagation of wave packets in one-dimensional PCs [5–7] confirmed the paradoxical theoretical conclusion about the convergence of the wave-packet delay time to some finite value, which is independent of the barrier thickness in the limit. The interpretation of superluminal tunnelling of a wave packet as reconstruction of its envelope [8] or propagation of its individual spectral components [9, 10] was heavily criticised [11, 12]. One of the most reasonable explanations of this paradox is that the tunnelling time is the release time of the energy stored in the barrier rather than the passage time through the barrier; within this concept, damped modes do not propagate in the barrier and can be considered as virtual photons that do not exist beyond the barrier [11, 18].

Analytical and numerical calculations of the wave-packet delay time in one-dimensional PCs were performed by different researchers [11, 19–21]. Note that the results of these studies are somewhat incomplete. The reason is that the main purpose was to explain the paradoxical dependence of the delay time, while some applied aspects of this problem were not considered. One of these aspects is the possibility of amplifying waves in PCs (for example, in active semiconductor heterostructures [22]) or the frequency modulation of propagating wave packet.

The purpose of our study was to calculate the propagation time of a frequency-modulated wave packet in an active PC, compare the derived expressions with the known results and discuss their potential applications.

## 2. Basic relations

Let us consider the propagation of waves in a one-dimensional PC (Fig. 1). For simplicity, we assume that the periodic change in the refractive index $n$ on a segment $[0, L]$ can be written as

$$n(z) = n_0 + n_1\cos(z/\Lambda). \quad (1)$$

This approximation describes fairly correctly a two-component PC with a step change in the refractive index of layers of the $n_0 - n_1$, $n_0 + n_1$ type, under small modulation ($n_1 \ll n_0$). Note that the condition of modulation smallness, being appropriate for most real PC structures, is not necessary and is used only to simplify calculations, making it possible to apply the coupled-wave analysis. Refractive-index modulation can also be set by a 'real' step profile, which only some-

**I.O. Zolotovskii, D.A. Korobko, V.A. Ostatochnikov** Ulyanovsk State University, ul. L'va Tolstogo 42, 432700 Ul'yanovsk, Russia; e-mail: korobkotam@rambler.ru, ost.vld@yandex.ru

Received 9 June 2014; revision received 20 July 2014
Kvantovaya Elektronika **45** (2) 136–142 (2015)
Translated by Yu.P. Sin'kov


**Figure 1.** Schematic diagram of wave propagation in an active one-dimensional PC.

what complicates the form of the coupling coefficient between waves [23]. The structure period $\Lambda$ determines the Bragg frequency for a given PC: $\omega_B = \pi c/(n_0\Lambda)$ (from here on, we limit our consideration by the region of the first-order Bragg reflection, where the band gap is maximal). The electric field in a one-dimensional PC can be presented as a superposition of waves propagating in opposite directions:

$$E(z) = A_1(z)\exp(-i\beta z) + A_2(z)\exp(i\beta z).$$

The incident wave $A_1(z)$, propagating along the $z$ axis, will be referred to as forward. The periodic change in the refractive index interrelates the initial forward wave with the backward wave $A_2(z)$, propagating in the opposite direction. The existence of gain in the system is taken into account by the increment $\alpha$. In this case, the dynamics of forward and backward waves can be described by the system of equations for their amplitudes [23]:

$$\begin{aligned}\frac{\partial A_1}{\partial z} - \alpha A_1 &= i\sigma A_2\exp(2i\delta z),\\ \frac{\partial A_2}{\partial z} + \alpha A_2 &= -i\sigma A_1\exp(-2i\delta z).\end{aligned} \tag{2}$$

Here, $\sigma$ is the coupling constant between the forward and backward waves, which can very easily be calculated for a harmonically changing refractive index (1): $\sigma = \pi n_1/\Lambda$; and $\delta = \beta - \pi/\Lambda = (\omega - \omega_B)n_0/c$ is the detuning from phase matching for oppositely directed waves. This form of equations takes into account that the propagation constant $\beta = n_0\omega/c$ when the modulation $n(z)$ is small. The boundary conditions for system (2) (a forward wave propagating along the $z$ axis) are set as $A_1(0) = A_0$, $A_2(L) = 0$; in this case, the solution to the system has the form [23, 24]

$$\begin{aligned}A_1(z) &= A_0\frac{s\cosh s(L-z) - (\alpha - i\delta)\sinh s(L-z)}{s\cosh sL - (\alpha - i\delta)\sinh sL}\exp(i\delta z),\\ A_2(z) &= A_0\frac{i\sigma\sinh s(L-z)}{s\cosh sL - (\alpha - i\delta)\sinh sL}\exp(-i\delta z),\end{aligned} \tag{3}$$

where $s = \sqrt{\sigma^2 + (\alpha - i\delta)^2}$. Complex transmittance $T$ and reflectance $R$ of the active photonic-crystal structure, defined at the ratios of the transmitted- and reflected-wave amplitudes to the input-wave amplitude, can be written as

$$\begin{aligned}T &= |T|\exp(-i\varphi_T')\\ &= \frac{A_1(L)\exp(-i\beta L)}{A_1(0)} = \frac{s\exp(-i\pi L/\Lambda)}{s\cosh sL - (\alpha - i\delta)\sinh sL},\end{aligned} \tag{4}$$

$$R = |R|\exp(-i\varphi_R') = \frac{A_2(0)}{A_1(0)} = \frac{-\sigma\sinh sL}{s\cosh sL - (\alpha - i\delta)\sinh sL}.$$

Expression (4) contains phases of complex reflectance and transmittance, $\varphi_R'$ and $\varphi_T'$, respectively. The spectral dependence of $T(\omega)$ and $R(\omega)$ is determined by their dependence on detuning $\delta$.

Let us now describe the transmission of a pulse with a time envelope $A(t)$ and carrier frequency $\omega_0$. An expression for the transmitted pulse envelope can be obtained using the inverse Fourier transform from the convolution of initial-pulse Fourier transform with complex transmittance $T(\omega)$:

$$A_T(t) = \frac{1}{2\pi}\int_{-\infty}^{\infty}\hat{A}_{in}(\Omega)\,T(\omega_0 + \Omega)\exp(i\Omega t)\,d\Omega, \tag{5}$$

where

$$\Omega = \omega - \omega_0;\ \hat{A}_{in}(\Omega) = \int_{-\infty}^{\infty}A(t)\exp(-i\Omega t)\,dt.$$

The complex transmittance has the form

$$T(\omega) = \exp(-i\Phi_T(\omega)) = \exp[-i(\varphi_T'(\omega)\ -i\varphi_T''(\omega))],$$

$$\varphi_T''(\omega) = -\ln|T(\omega)|.$$

Approximate expressions for $A_T(t)$ and the delay time for a pulse transmitted through a PC can be derived by expanding $T(\omega)$ in a Taylor series in the vicinity of the carrier pulse frequency $\omega_0$. Let us introduce some designations to use below, based on the fact that

$$\begin{aligned}\Phi_T(\omega) &\approx \Phi_T(\omega_0) + \left.\frac{\partial(\varphi_T' - i\varphi_T'')}{\partial\omega}\right|_{\omega=\omega_0}(\omega - \omega_0)\\ &+ \frac{1}{2}\left.\frac{\partial^2(\varphi_T' - i\varphi_T'')}{\partial\omega^2}\right|_{\omega=\omega_0}(\omega - \omega_0)^2 + \ldots\\ &= \Phi_T(\omega_0) + (K_r + iK_i)\,\Omega + \frac{1}{2}(D_r + iD_i)\,\Omega^2 + \ldots.\end{aligned}$$

We calculate the delay time on the assumption that the initial Gaussian pulse has a linear frequency modulation (chirp) $C$:

$$A(t) = A_0\exp[-(1 + iC)\,t^2/2\tau_0^2], \tag{6}$$

where $\tau_0$ is the pulse duration and chirp $C = a\tau_0^2$; the frequency modulation rate along the pulse is constant: $a(t) = \text{const}$. In this case, the expression for the transmitted-pulse envelope $A_T(t)$, obtained by neglecting terms of an order higher than the second one in the Taylor series, has a Gaussian form [25–27]:

$$A_T(t) = \rho(t)\exp[i\phi(t)], \tag{7}$$

where

$$\rho(t) = A_0\,|T(\omega_0)|\exp\left[K_i^2(1 + S^2)\tau_p^{-2}\right]\left(\frac{\tau_0}{\tau_p}\right)^{1/2}\exp\left[-\left(\frac{\tau_s}{\tau_p}\right)^2\right];$$

$$2\phi(t) = \frac{S\tau_s^2 + 2\tau_s K_i(1 + S^2) + K_i^2 S(1 + S)}{\tau_p^2}$$

$$- \arctan(S + C) - 2\varphi_T'(\omega_0).$$

Here, we introduced (using parameters $\chi_1 = (CD_r - D_i)\tau_0^{-2}$ and $\chi_2 = (CD_i + D_r)\tau_0^{-2}$ the duration of transmitted pulse:

$$\tau_p = \tau_0^2\left[\frac{(1-\chi_1)^2+\chi_2^2}{\tau_0^2+D_i(1+C^2)}\right]^{1/2}. \quad (8)$$

We introduced also the parameter

$$S = \frac{(1+C^2)D_r - C\tau_0^2}{(1+C^2)D_i+\tau_0^2} = \left[(1+C^2)\frac{\partial^2\varphi'_T}{\partial\omega^2}\bigg|_{\omega=\omega_0} - C\tau_0^2\right]$$
$$\times\left[\tau_0^2-(1+C^2)\frac{\partial^2\ln|T|}{\partial\omega^2}\bigg|_{\omega=\omega_0}\right]^{-1}, \quad (9)$$

which depends on not only the characteristics of the PC band gap but also on the duration and frequency modulation of the pulse. When considering the transmission of pulses with an initial chirp, the $S$ value is of key importance.

The shift ($\tau_s$) of the maximum of the pulse envelope,

$$\tau_s = t - K_r(\omega_0) - SK_i(\omega_0)$$
$$= t - \frac{\partial\varphi'_T}{\partial\omega}\bigg|_{\omega=\omega_0} - S\frac{\partial\ln|T|}{\partial\omega}\bigg|_{\omega=\omega_0} \quad (10)$$

is of greatest interest when solving the problem of pulse delay in a PC.

The position of the pulse carrier frequency in the spectrum of the PC band gap determines to a great extent the shift of the pulse maximum. Time $\tau_s$ is an analogue of time in the related coordinate system in an extended dispersive medium: $\tau = t - z/v_g$, where $v_g = \partial\omega/\partial\beta$ is the group velocity. The delay time of a pulse transmitted through a PC was calculated in [11, 19–21] with allowance for only one term. This approach holds true for non-chirped pulses ($C = 0$) and far from the band gap edges [at $(\partial\ln|T|/\partial\omega)|_{\omega=\omega_0} \to 0$]. In this case, the delay time

$$\tau_d = (\partial\varphi'_T/\partial\omega)|_{\omega=\omega_0}. \quad (11)$$

To illustrate the above considerations, we will derive an expression for $\tau_d$ from formulas (4) in the case of a passive ($\alpha = 0$) PC, within its band gap ($\delta < \sigma$). Here,

$$\varphi'_T = \arctan(\delta\tanh(sL)/s).$$

According to (11), the delay time is [18]

$$\tau_d = \frac{n_0 L}{c}\left[\frac{(\sigma/s)^2\tanh(sL)/sL - (\delta/s)^2\operatorname{sech}^2(sL)}{1+(\delta/s)^2\tanh^2(sL)}\right]. \quad (12)$$

When considering extremely wide barriers ($L \to \infty$), one arrives at a paradoxical conclusion that the delay time converges to a finite value $\tau_d = n_0/sc$; the expression is especially simple in the middle of the band gap (at $\delta = 0$): $\tau_d = n_0/\sigma c = \Omega_c^{-1}$, where $\Omega_c$ is the band gap width. The paradox related to the infinite tunnelling velocity is solved if the delay time is not considered as the pulse transmission time through the barrier. The spatial 'size' of the pulse exceeds the barrier thickness $L$, and the pulse propagates quasi-statically. As a result, the field distribution in the barrier is stationary. In this context, the PC is similar to a capacitor, and the delay time is the ratio of the average accumulated energy to the introduced power [28]. The energy of the radiation with a spectrum lying within the band gap is concentrated near the barrier surface, and its density rapidly (almost exponentially) decreases over the barrier length. In the example of a passive PC considered above, the radiation energy density at the Bragg wavelength ($\delta = 0$) is distributed over the PC length:

$$\langle u\rangle = n_0^2 A_0^2\frac{\cosh[2\sigma(z-L)]}{2\cosh^2(\sigma L)}.$$

Hence, at sufficiently large $L$ values, the energy accumulated in a PC is rapidly saturated with length according to the law $\propto\tanh\sigma L$. Specifically this circumstance explains the saturation of delay time $\tau_d$, i.e., the Hartman paradox. An interested reader may also refer to review [11] and references therein, where experiments aimed at verifying the Hartman paradox are described in detail and the arguments of all participants of the discussion are analysed.

## 3. Delay time in active photonic crystals

When considering the delay time $\tau_d$ for active PCs, one should take into account that the introduction of gain does not change radically the dependence of the delay time $\tau_d$ in the middle of the band gap on the barrier width. Bragg reflection excludes penetration of radiation with frequencies $\omega \approx \omega_B$ deep into the structure, and the so-called energy capacitance of a PC barely changes at these frequencies. Specifically this circumstance leads to conservation of $\tau_d$. At the same time, one can observe interesting effects near the band gap edges at $\delta \to \sigma$, which are related to the change in $\tau_d$. Since we consider the transmission of a pulse with a carrier frequency near the band gap edge, the derivative $(\partial\ln|T|/\partial\omega)|_{\omega=\omega_0}$ cannot be equated to zero and, strictly speaking, one must apply a more general expression (10) to calculate the delay time in this case. However, $|S| \ll 1$ for a pulse without frequency modulation, and the delay time for the maximum of the transmitted pulse can be estimated from the standard formula $\tau_d = (\partial\varphi'_T/\partial\omega)|_{\omega=\omega_0}$.

Figure 2 shows spectral dependences of transmittance modulus $|T|$ and delay time (11), calculated for active PC structures with the following parameters: $n_0 = 3$ and $2n_1 = 0.015$. The aforementioned values are close to the parameters of widespread semiconductor structures based on $Al_{0.7}Ga_{0.3}As$ at frequency $\omega_B$, which corresponds to a wavelength of about 1.5 μm [29].

For a passive PC (dashed curves in Fig. 2), one can show, proceeding from (12), that, at $\delta \to \sigma$, the delay time increases to the value equal to the PC transmission time for a wave with a velocity equal to the speed of light in the medium: $\tau_d = n_0 L/c$. An introduction of gain leads to a sharp increase in parameter $\tau_d$ in a narrow ($\delta \approx \sigma$) spectral band [curve (*1*)]. This effect is explained by the rather deep penetration of radiation at this frequency into the structure, multiple rereflection in this band and increase in the PC energy capacitance. This spectral region contains a singularity of complex transmittance $T(\omega)$, at which the denominator of expressions (4) becomes zero. At this point $|T| \to \infty$, and the energy release in the structure does not call for the input radiation; i.e., generation occurs. Each singularity corresponds to one of the distributed-feedback (DFB) laser modes [23]. Note that the delay time increases to infinity at the generation point, because the PC structure emits at the zero introduced energy.

One can see that an increase in gain [Fig. 2, curve (*2*)] makes the singularity of the coefficient $T(\omega)$ pass to the range $\delta > \sigma$; i.e., the next modes of the DFB laser have a larger detuning and are excited at a higher gain. It is noteworthy that phase $\varphi'_T$ rapidly changes in the frequency range before the singularity, and its derivative $\partial\varphi'_T/\partial\omega$ may change sign;

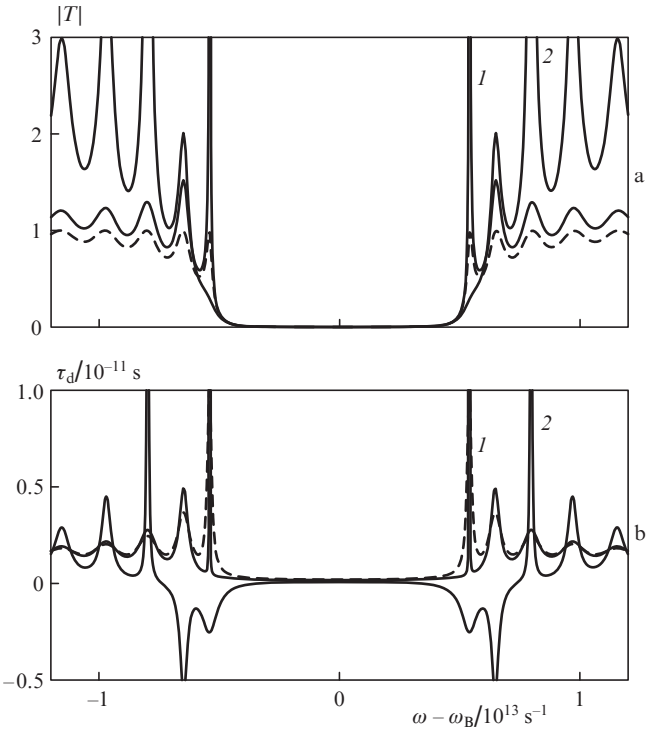


**Figure 2.** (a) Modulus of transmittance (4) for a PC structure with $\sigma = 5\times10^4$ m$^{-1}$ and $L = 150$ μm and (b) delay time $\tau_d$, calculated according to (11) for the aforementioned structures, at gains $\alpha L = (1)\ 0.15$ and $(2)$ 0.75. The dashed curves are the dependences for a passive PC ($\alpha = 0$).

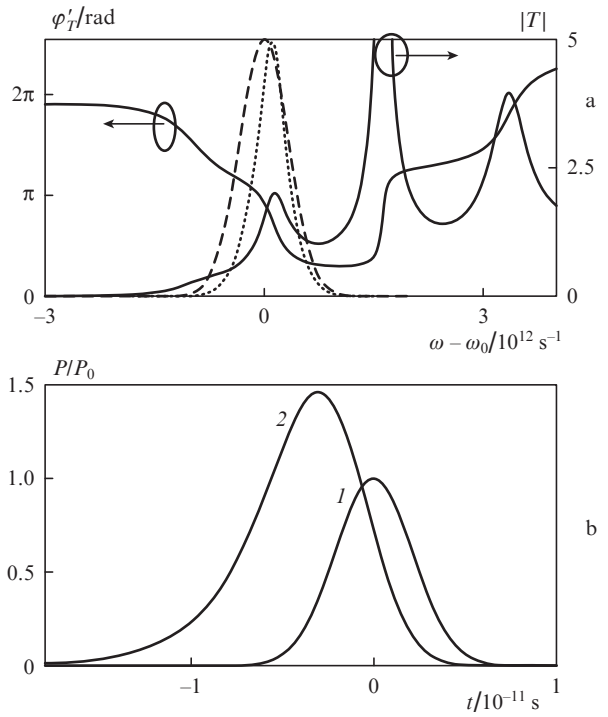


**Figure 3.** (a) Phase and modulus of transmittance (4) for a PC structure with $\sigma = 5\times10^4$ m$^{-1}$, $L = 150$ μm, and $\alpha L = 0.75$ (the moduli of the spectra of input and transmitted pulses $|\hat{A}(\Omega)|$, normalised to the maximum value, are shown by dashed and dotted lines, respectively). (b) Envelopes of the $(1)$ input pulse, $|A(t)|^2$, and $(2)$ pulse transmitted through an active PC structure, $|A_T(t)|^2$.

i.e., there may be negative $\tau_d$ values. This phenomenon, which is rather typical of wave propagation in active media [30, 31], is in no way related to the violation of the causality principle and can be clarified by the following considerations. The mean energy, stored in a PC structure with a cross-sectional area $b^2$,

$$\langle U\rangle = \frac{n_0^2 b^2}{2}\int_0^L (|A_1|^2 + |A_2|^2)\,\mathrm{d}z,$$

is rapidly saturated with length $L$ [in the range of finite values $T(\omega)$, $R(\omega) < \infty$]. When the detuning and gain level satisfy a certain relation, the PC energy capacitance is insufficient for storing the energy generated in the structure. Actually, we see that the radiation is 'pushed out' from the PC.

This consideration is illustrated by Fig. 3, which shows the results of direct numerical simulation of system (5) for the above-discussed active PC structure with $\alpha L = 0.75$. The spectrum of the initial Gaussian pulse with a duration $\tau_0 = 3\times10^{-12}$ s lies in the range of negative values of the derivative $\partial\varphi'_T/\partial\omega$. High-power gain leads to a fast rise of the leading edge of the transmitted pulse [Fig 3b, curve $(2)$]. The top of the transmitted pulse is shifted toward negative times, i.e., to the 'future' with respect to the input-pulse maximum. The limited PC energy capacitance leads to the following effect: the maximum of the transmitted pulse is formed when the input-pulse maximum is still beyond the PC. This phenomenon is a striking example of envelope transformation [8, 30, 31]. The transmitted pulse spectrum (Fig. 3a, dotted curve) does not contain any low-frequency components of the initial pulse (the dashed curve). Thus, the transmitted pulse maps only partially the input pulse, and there is no 'superluminal' data transfer.

## 4. Delay time of frequency-modulated pulses in a one-dimensional photonic crystal

Let us consider again the expression for the shift $\tau_s$ of the pulse envelope maximum (10). Until now, our consideration was limited by the first term on the right-hand side of this expression. The radiation delay was provided by the dispersion dependence of the transmittance phase $\tau_d = (\partial\varphi'_T/\partial\omega)|_{\omega=\omega_0}$. With due regard to the term $-S\partial\ln|T|/\partial\omega|_{\omega=\omega_0}$, one can note that the displacement time of the transmitted-pulse maximum is determined not only by the PC structure parameters but also by the pulse characteristics, in particular its frequency modulation (chirp).

In this part of the study we investigated the influence of the chirp of the input pulse on its output parameters, including the delay time $\tau_s$ of the pulse maximum. To this end, we performed direct numerical simulation of system (5) for the input Gaussian pulse (6) with a duration $\tau_0 = 10^{-7}$ s and linear frequency modulation $C = 2\times10^4$. For comparison, a similar numerical solution was performed for an initial Gaussian pulse of the same spectral width but without frequency modulation. Its duration was $\tau'_0 = \tau_0(1 + C^2)^{-1/2} \approx \tau_0/C = 5\times10^{-12}$ s.

To exclude generation, the calculated gain parameter of the active PC was chosen to be smaller than in the example considered above, while the other PC-structure parameters were the same. The pulse carrier frequency $\omega_0$ was chosen so as to correspond to the PC band gap edge.

Figure 4 shows normalised spectral power densities for the input and transmitted pulses, as well as the spectral dependence of transmittance modulus $|T|$ (dashed line). Since the transmitted pulse spectrum is determined by the convolution of the input pulse spectrum with the PC transmission spec-

trum, $\hat{A}_{out}(\Omega) = \hat{A}_{in}(\Omega)\,T(\Omega)$, coincidence of spectral densities of the non-chirped and chirped pulses, $|\hat{A}_{in}(\Omega)|$, leads to coincidence of the spectral densities of transmitted pulses, $|\hat{A}_{out}(\Omega)|$. Thus, pulses having different chirps but equal spectral widths cannot be distinguished in Fig. 4. Nevertheless, the difference in the phase dependences $\hat{A}_{in}(\Omega)$ leads to significantly different envelopes of transmitted pulses, $|A_T(t)|^2$ (see Fig. 5).

It can be seen in Fig. 4 that both chirped and non-chirped pulses have initially frequency components that are amplified in the active PC structure. In the case of chirped pulse (Figs 5a, 5b), these components propagate at the leading edge of the long input pulse. The transmitted pulse, retaining the initial frequency modulation, loses the PC-filtered low-frequency components. As a result, one can see that the maximum of the transmitted pulse is located before the maximum of the input pulse; i.e., a negative pulse delay occurs again. In contrast to the previous case (Fig. 3), the envelope transformation is caused by not only the gain in the PC structure, but basically by filtering the components distributed over the pulse length. In the case of inverse linear frequency modulation ($C < 0$), a positive delay is observed, which is related to suppression of the leading edge and rise of the trailing edge of the pulse. Since the delay depends on chirp $C$, it cannot be described using only expression (11). As the first approximation, one can apply expression (10). It is of importance that the transmitted pulse is much shorter than the input one. This effect can only arbitrarily be referred to as compression, because the transmitted pulse does not completely maps the input one. The compression is due to the fact that the transmitted frequency band is concentrated in a narrow time interval at the leading edge of the pulse.

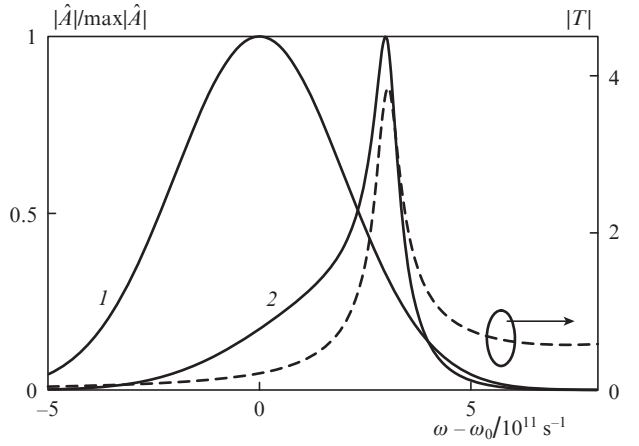


**Figure 4.** Normalised (to maximum) spectral densities $|\hat{A}(\Omega)|/\max|\hat{A}(\Omega)|$ of the (*1*) input (chirped and non-chirped) pulses and (*2*) a pulse transmitted through a PC structure with $\sigma = 5\times10^4$ m$^{-1}$, $L = 150$ μm, and $\alpha L = 0.1125$. The dashed line is the spectral dependence of the modulus of PC structure transmittance $|T(\omega)|$. The difference between the carrier frequency of the input pulse and the frequency at the middle of the band gap is $\omega_0 - \omega_B = 5.1\times10^{12}$ s$^{-1}$.

Concerning the transmission of a shorter but initially non-chirped pulse (Figs 5c, 5d), it should be noted that its delay is determined by only the dispersion of complex transmittance $T(\omega)$. The transmitted spectral components are uniformly distributed over the input pulse length. During multiple rereflections in the PC structure, these components are selected from the initial spectrum to form the transmitted pulse. Due to the dispersion dependence $T(\omega)$, the transmitted pulse undergoes a dispersion spread and becomes frequency-modulated. The significant spectral narrowing of the transmitted pulse (in comparison with the input one), along with the dispersion spread, leads to a decrease in the peak power and an increase in the transmitted pulse duration. As was mentioned above, the delay time of the transmitted pulse maximum in the absence of initial chirp can be estimated (even at the band gap edge) based on standard formula (11). Indeed, in the case under consideration, the governing parameters $(\partial\ln|T|/\partial\omega)|_{\omega=\omega_0}$ and $S$ are, respectively, $\sim4.7\times10^{-12}$ s and $\sim0.08$, and correction $S(\partial\ln|T|/\partial\omega)|_{\omega=\omega_0}$ does not exceed few percent of $(\partial\varphi'_T/\partial\omega)|_{\omega=\omega_0}$.

Then we will consider the dependence of transmitted pulse characteristics on the initial chirp. The results of numerical calculations for a PC structure with the parameters indicated in Fig. 4 and an input Gaussian pulse with duration $\tau_0 = 10^{-7}$ s are presented in Figs 6 and 7. In accordance with the aforesaid, one can see that pulses with positive and negative chirps are characterised by negative and positive delays, respectively. Several regions of values of input pulse chirp $C$ with similar transmitted pulse characteristics can be selected. In the central region in Fig. 6 (in our case, $|C| < 1.85\times10^4$), the input pulse spectrum with width $\Delta\omega_s \approx C/\tau_0$ lies mainly within the band gap. The peak power of the transmitted pulse is much lower than the input pulse power. The formation of its envelope is affected by two factors: dispersion shift of the tunnelling Gaussian pulse and transmission of the frequency components corresponding to the transmission band and compactly concentrated at one of the input pulse edges (Fig. 4). In both cases the pulse chirp plays a key role. When describing the shift of the maximum of chirped pulses, the third term in expression (10), $S(\partial\ln|T|/\partial\omega)|_{\omega=\omega_0}$, becomes determining at $|C| > 100$. The pulse shift proportional to $\partial\varphi'_T/\partial\omega$ is independent of chirp and small [in the case under study it is about $10^{-12}$ s (see Fig. 5d)].

In the middle of the central region the factor related to the dispersion shift of the entire spectrum of chirped tunnelling pulse is dominant. In this case the transmitted pulse retains a Gaussian shape and is negatively and positively delayed at $C > 0$ and $C < 0$, respectively. With an increase in $|C|$, the frac-

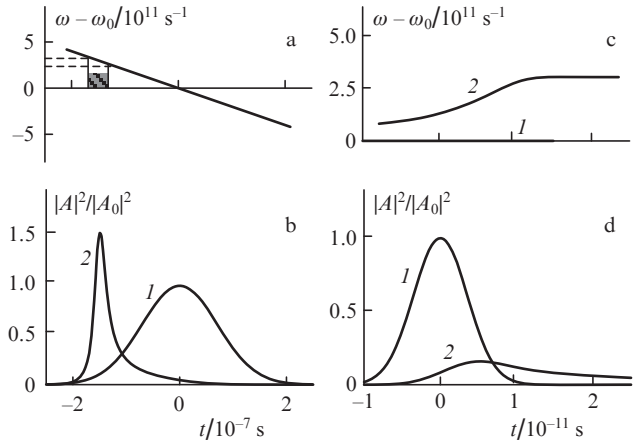


**Figure 5.** (a) Instantaneous frequency of the chirped input and transmitted pulses (the dark area is the region of compact location of the transmitted spectral components), (b) envelopes of the (*1*) chirped and (*2*) transmitted pulses, (c) instantaneous frequency of the (*1*) non-chirped input pulse and (*2*) transmitted pulse, and (d) the envelopes of the (*1*) non-chirped input pulse and (*2*) transmitted pulse.

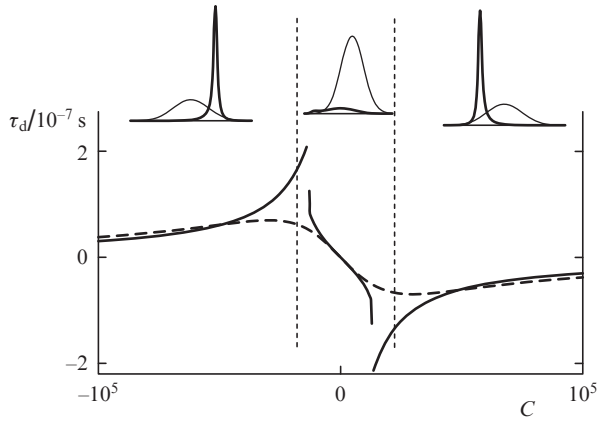


**Figure 6.** Dependence of delay time $\tau_d$ of initially chirped pulse in an active PC structure on chirp $C$. The solid lines are the result of a numerical calculation according to system (5) and the dashed line is the result of a calculation based on (10). An input pulse (thin solid lines) and a pulse transmitted through the PC structure (bold lines), typical of each region of initial chirp values, are shown in a simplified form in the top.

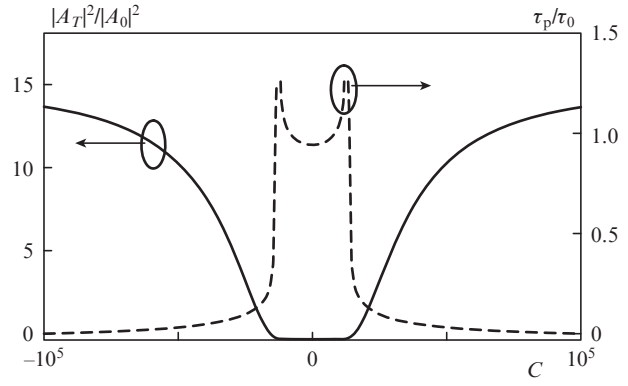


**Figure 7.** Ratios of the peak powers (solid line) and durations (dashed line) of transmitted and input pulses.

tion of the transmitted spectral components concentrated in a narrow part of the input-pulse leading edge increases. This effect leads to distortion of the transmitted pulse and formation of the second peak in it. The region of discontinuities in Fig. 6 corresponds to equalisation of powers in the peaks of the transmitted pulse. Note that analytical solution (10) cannot be applied in this region, because the initial assumption that the shape of the transmitted pulse envelope is close to Gaussian (7) is not valid in principle because of the complex pulse distortion. The approach based on parabolic approximation of spectrum $T(\omega)$ expanded in a series has limited applicability in this case.

With a further increase in $|C|$ the maximum of the transmitted pulse is related to only the second factor: transmission and amplification of the frequency band concentrated at one of the input pulse edges; the influence of the first factor becomes insignificant. The boundaries of the central region in Fig. 6 correspond arbitrarily to the chirp values at which the peak power of the transmitted pulse is equal to the input-pulse peak power. In the regions of strong frequency modulation (in our case, where $|C| > 1.85\times10^4$), one can see that the shift magnitude decreases with an increase in $|C|$. This can be explained by the fact that, with an increase in chirp, the time coordinate of the transmitted frequency components tends to the input pulse maximum $t = 0$. It is noteworthy that the transmitted pulse envelope takes again a shape close to symmetric Gaussian, and analytical expression (10), beginning with a certain $|C|$ value, describes quite adequately the transmitted-pulse delay time.

Figure 7 shows the results of numerical calculations according to (5), which illustrate the compression of the transmitted pulse with respect to the input one. As in Fig. 6, one can select a region of $C$ values in which the transmitted pulse characteristics are determined by different factors. In the central region, at small $|C|$, the input pulse spectrum lies within the band gap; in this case, the peak power and energy of the tunnelling pulse are low. Its behaviour is determined by the dispersion spread, due to which the transmitted pulse duration exceeds the duration of the input pulse.

The situation radically changes with an increase in $|C|$. As was mentioned above, the input pulse spectrum is now characterised by a higher intensity of the components falling in the transmission band and compactly concentrated at one of the pulse edges. This leads to the formation of a transmitted pulse with a high peak power and low duration, corresponding to the transmitted components. A further increase in $|C|$ is accompanied by an increase in both the density of transmitted components (proportionally to $|C|$) and their intensity, because the region of their compact location approaches the input pulse maximum. As a result, the transmitted pulse undergoes compression, which increases with an increase in $|C|$. The compression saturation at very large chirp values, which is pronounced in Fig. 7, is due to the fact that the spectrum of the frequency-modulated input pulse becomes very wide, and its larger part falls not only in the narrow transmission band at the band gap edge but also covers the region of low spectral contrast $T(\omega)$ (see Fig. 2). The dispersion factors, which accompany transmission in these regions, reduce the intensity of the spectral components in the narrow transmission band.

## 5. Conclusions

The main purpose of our study was to expand the description of pulse transmission in one-dimensional PCs in order to consider the propagation of frequency-modulated pulses in PCs with gain. The emphasis was on the transmission of pulses with a spectrum located within the PC band gap. Based on the general approach, we obtained an expression for the time delay of the transmitted pulse maximum with respect to the initial pulse maximum. As the analysis showed, the obtained expression (10) refines the standard formula (11), which is used to calculate the delay time in one-dimensional PCs. The standard consideration leaves completely aside the pulse characteristics: its duration and frequency modulation, as well as the position of the pulse spectrum in the band gap. The derived expression (10) describes correctly the shift of the transmitted pulse maximum with due regard to these effects.

The analytical calculations were supplemented with a numerical simulation of the process under study. The results of this simulation, being in fundamental agreement with the theory, demonstrate the importance of considering the frequency modulation of the input pulse, the position of its spectrum in the band gap, and the gain in the PC structure. In particular, it was shown that the PC-structure gain may lead to the occurrence of the so-called negative delay time, caused

by the transformation of the input pulse envelope (even in the absence of frequency modulation).

The main results of the study are related to the obtained dependences of the transmitted pulse characteristics (delay time, duration, and peak power) on the input pulse chirp. It was shown that, changing the chirp, one can control the transmitted-pulse delay time and implement, in particular, both negative and positive delays. It is also important that pulses with peak power and duration depending on the initial chirp can be formed.

The practical importance of this study is related to the possibility of developing a series of optoelectronic devices for radiation control. We believe devices with controlled pulse delay, which are necessary for different optoelectronic schemes, to be most promising. These devices can be based on semiconductor heterostructures with optical or electrical pumping.

***Acknowledgements.*** This work was supported by the Ministry of Education and Science of the Russian Federation (Project No. 14.Z50.31. 0015 and State Contract). V.A. Ostatochnikov acknowledges the 'Support for Research' programme.

## References

1. MacColl L.A. *Phys. Rev.*, **40**, 621 (1932).
2. Shvartsburg A.B. *Usp. Fiz. Nauk*, **177**, 43 (2007).
3. Hartman T.E. *J. Appl. Phys.*, **33**, 3427 (1962).
4. Olkhovsky V.S., Recami E. *Phys. Rep.*, **214**, 339 (1992).
5. Spielmann Ch., Szipöcs R., Stingl A., Krausz F. *Phys. Rev. Lett.*, **73**, 2308 (1994).
6. Longhi S., Marano M., Laporta P. *Phys. Rev. E*, **64**, 055602 (2001).
7. Hache A., Poirier L. *Appl. Phys. Lett.*, **80**, 518 (2002).
8. Chiao R.Y., Steinberg A.M., in *Progress in Optics*, Vol. XXXVII (Amsterdam: Elsevier, 1997) p. 345.
9. Buttiker M. *Phys. Rev. B*, **27**, 6178 (1983).
10. Landauer R. *Sol. State Commun.*, **84**, 115 (1992).
11. Winful H. *Phys. Rep.*, **436** (1-2), 1 (2006).
12. Winful H.G. *IEEE J. Sel. Top. Quantum Electron.*, **9**, 17 (2003).
13. Bigelow M.S., Lepeshkin N.N., Boyd R.W. *Science*, **301**, 200 (2003).
14. Vlasov Y.A., O'Boyle M., Hamann H.F., McNab S.J. *Nature*, **438**, 65 (2005).
15. Inoue K., Ohtaka K. *Photonic Crystals: Physics, Fabrication and Applications* (Berlin: Springer, 2010).
16. Sakoda K. *Optical Properties of Photonic Crystals* (Berlin: Springer, 2001).
17. Steel M.J., Levy M., Osgood R.M. *IEEE Photon. Technol. Lett.*, **12**, 1171 (2000).
18. Winful H.G. *New J. Phys.*, **8**, 101 (2006).
19. Esposito S. *Phys. Rev. E*, **64**, 026609 (2001).
20. Pereyra P., Simanjuntak H.P. *Phys. Rev. E*, **75**, 056604 (2007).
21. Endo R., Saito R. *J. Opt. Soc. Am. B*, **28**, 2537 (2011).
22. Alferov Zh.I. *Fiz. Tekh. Poluprovodn.*, **32**, 3 (1998).
23. Yariv A. *Introduction to Optical Electronics* (New York: Holt, Rinehart, and Winston, 1976; Moscow: Vysshaya shkola, 1983).
24. Yariv A., Yen H.W. *Opt. Commun.*, **10**, 120 (1975); Wang S. *J. Appl. Phys.*, **44**, 767 (1973).
25. Zolotovskii I.O., Sementsov D.I. *Kvantovaya Elektron.*, **34**, 852 (2004) [*Quantum Electron.*, **34**, 852 (2004)].
26. Zolotovskii I.O., Sementsov D.I. *Opt. Spektrosk.*, **99**, 89 (2005).
27. Zolotovskii I.O., Sementsov D.I. *Kvantovaya Elektron.*, **37**, 187 (2007) [*Quantum Electron.*, **37**, 187 (2007)].
28. Winful H. *Opt. Express*, **10**, 1491 (2002).
29. Pikhtin A.N., Yas'kov A.D. *Sov. Phys. Semicond.*, **14**, 389 (1980).
30. Oraevskii A.N. *Usp. Fiz. Nauk*, **41**, 1199 (1998).
31. Bukhman N.S. *Kvantovaya Elektron.*, **34**, 120 (2004) [*Quantum Electron.*, **34**, 120 (2004)].